

## CRACK TORTUOSITY IN SWELLING CLAY SOILS\*

*V.Y. Chertkov, I. Ravina*

Faculty of Agricultural Engineering, Technion, Haifa 32000, Israel

*Accepted February 17, 1998*

**A b s t r a c t.** A relationship between the planar and spatial tortuosities of a statistically isotropic crack network in a clay soil is derived from the fact that connected cracks outline peds and are their boundaries. Connectedness, a parameter characterizing the crack network, determines this relationship. The two- and three-dimensional tortuosities vary from 1.5 to 2.2 and from 1.4 to 3.25, respectively, when connectedness decreases from unity to zero. A method proposed for processing two-dimensional images of crack networks enabled the estimation of two- and three-dimensional tortuosities of an assumed isotropic crack network. Two-dimensional images of seventeen different crack networks, available in the literature, were used to show the application of the proposed dependency between planar and spatial tortuosities.

**K e y w o r d s:** swelling soil, crack network, crack connectedness, planar tortuosity, spatial tortuosity

### INTRODUCTION

One of the characteristics of a crack network in a clay soil is tortuosity which determines the mean length of flow through cracks and influences the hydraulic properties of the soil. Tortuosity definition of crack network can be introduced either as planar tortuosity of a two-dimensional crack network of linear cracks on a soil cross-section or as spatial tortuosity of a three-dimensional crack network of planar cracks. The main purpose of this work is to show that, in the case of a statistically isotropic crack network, there is a relationship between the

planar and the spatial tortuosities. It is clear that to estimate experimentally the planar tortuosity from a two-dimensional image of a crack network is much simpler than to estimate the spatial tortuosity from a three-dimensional image. So the relationship may be used for estimation of the spatial tortuosity from the planar one.

First we define the tortuosities of the crack network in the two- and three-dimensional cases. Then we calculate them as functions of each other on the basis of the distribution of ped dimensions and show how to estimate them from an experimental two-dimensional image of a crack network which is assumed to be statistically isotropic. To evaluate the model we used crack network images available in literature.

### THEORY

One may consider the crack network in a sufficiently small volume, as well as in any of its cross-sections, as statistically homogeneous. The crack network is characterized by a dimensionless value,  $c$  describing the extent of the crack coalescence (the crack network connectedness) and by an average spacing between crack intersections with a straight line,  $d$  [1, 2, 4]. The connectedness,  $c_2$  for a cross-sectional plane of the crack network may depend on its

---

\*Paper presented at 6 ICA

orientation and differ from the spatial crack network connectedness,  $c_3$  because natural crack networks can be anisotropic [14]. For simplicity, we shall assume that crack networks are locally isotropic when  $c_2$  does not depend on the orientation of the cross-section. In the isotropic and homogeneous case the connectedness  $c_3$  may differ from the connectedness  $c_2$  only because of cracks coplanar with the cross-section under consideration. However, it may be assumed that the number of these is very small compared with the number of cracks intersecting the cross-section, and one may consider  $c_2 = c_3 \equiv c$ . In the following, results based on the assumption of local crack network isotropy will be compared with experimental data.

In the two dimensional (planar) case, the tortuosity of a crack network,  $T_2$  is defined as:

$$T_2 = L_2 / L_1 \quad (1)$$

where  $L_1$  is the number of cracks intersecting the side of a unit square and which are connected with other cracks within it forming continuous through (linear) paths to the opposite side (in the following, straight sections of such a path are referred to as (one dimensional) through-connected cracks);  $L_2$  is the total length of through-connected cracks per unit area. Similarly in the three-dimensional case the tortuosity of a (spatial) crack network,  $T_3$  is defined as:

$$T_3 = L_3 / L_2 \quad (2)$$

where  $L_2$  is the total length of the traces of cracks intersecting the side of a unit cube and connected with cracks within it forming continuous, through (areal) paths to its opposite side (in the following planar sections of such paths are referred to as (two dimensional) through-connected cracks);  $L_3$  is the total surface area of the through-connected cracks per unit volume.

The key point of the approach to estimate the values of  $L_1$ ,  $L_2$  and  $L_3$  is: connected cracks outline, or nearly outline, peds and are their boundaries. Consequently  $L_1$ ,  $L_2$ , and  $L_3$  may be estimated from the distributions of fragment dimensions in the one-, two- and three-dimensional cases, respectively ("a one dimensional fragment" is the spacing between intersections

with a line of two neighboring connected cracks). Using the distributions derived from the model of multiple cracking and fragmentation [1,2,4], with the parameters: connectedness,  $c$  and mean crack spacing,  $d$  one can get the expression:

$$L_n = B_n(c) / d, \quad n = 1, 2, 3 \quad (3)$$

where  $B_n(c)$  are dimensionless functions of the connectedness. According to Eqs (1), (2) and (3) the tortuosities are:

$$T_n(c) = B_n(c) / B_{n-1}(c), \quad n = 2, 3. \quad (4)$$

Equation (4) (for  $n = 2$  and  $3$ ) shows that the tortuosity  $T_3$ , as well as the tortuosity  $T_2$ , do not depend on the scale factor (the mean spacing between cracks)  $d$ , but only on the connectedness  $c$  as the parameter of crack network. It is assumed that the shape of a two- or a three-dimensional fragment is, on the average, a square or a cube, respectively. The line in Fig. 1 shows the dependency  $T_3(T_2)$  resulting from the dependencies  $T_2(c)$  and  $T_3(c)$  for an isotropic and homogeneous crack network. As can be seen, the tortuosity  $T_3$  increases from 1.4 to 3.25 and the tortuosity  $T_2$  from 1.5 to 2.2 when the connectedness  $c$  decreases from one to zero.

## MATERIALS AND METHODS

In this work we are interested in finding tortuosities  $T_2$  and  $T_3$  from two-dimensional images of crack networks. The images of crack networks can be: a) at the soil surface; b) at different cross-sections of soil cores or blocks; and c) at the surface of specially-prepared soil samples. A number of such images are available in the literature [7,9-14] and were used for evaluation of the model. They are shown in Fig. 2 on a much smaller scale than the originals. They are numbered according to decreasing connectedness. Images 1-4, 6, 9, 11, 13 (from Fig. 2 of Guidi *et al.* [7]) are photographs of eight replicates of artificially-prepared samples of the 1-2 mm fractions of an Italian Fluvisol, >48% clay (images 1-4) and a Regosol, >46% clay (images 6, 9, 11, 13). Image 5 from Ringrose-Voase and Bullock ([10], Fig. 4(c)) is a photograph of a horizontal cross-section of a Windsor soil, at

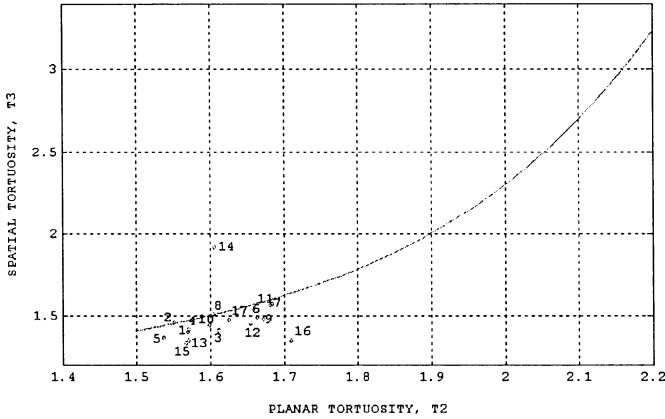


Fig. 1. Predicted mean three-dimensional tortuosity  $T_3$  of an isotropic crack network as a function of the two-dimensional tortuosity  $T_2$  (solid line) and experimental data (points) of clay soils (the numbers refer to soils shown in Fig. 2).

depth 46 cm. Images 7 and 12 are Fig. 7 and the lower part of Fig. 1, respectively, of Scott *et al.* [13]; they are photographs of horizontal cross-sections of clayey subsoils of the Swanwick series at a depth of 46 cm and of the Windsor series at a depth of 35 cm, respectively. Images 8 and 16 are Fig. 1( $\frac{V}{3}$ ) and Fig. 1( $\frac{S}{9}$ ), respectively, of Ringrose-Voase and Nys [11]; they are photographs of 12.7x10.16 cm horizontal cross-sections of a blocky and a prismatic soil sample, respectively, from North Wales at a depth of 7 cm. Image 10 is Fig. 1 of Ringrose-Voase [9] of a cross-section of a soil from Wales. Images 14 and 15 are two parts of Fig. 1 of Scott *et al.* [12]; the photographs are of 4.8x7.2 cm soil thin sections cut at random angles of both elevation and azimuth from a profile of the Windsor-series-of-London clay in Essex at depth 35 cm. Image 17 is the right part of Fig. 4(b) of Velde *et al.* [14] which is a photograph of a 5x10 cm soil vertical thin section from a vertisol profile (>65% clay) in Southern Italy at a depth of 155 cm.

The procedure of preparing the images was as follows:

- the original image was magnified to a linear dimension of ~20 cm;
- a strip of the boundary of the magnified image, ~1.5 cm wide, was excluded if it was distorted to allow to get a "working window" square of a side length of 14-23 cm;

- a grid with a spacing of 1 cm was drawn on the working window (we designated the total number of the horizontal and vertical lines by  $i_0$ ).

In the image working window, a line section is considered to be *the trace of a spatial crack* if the ratio of its length to width is 3 and the length is 2 mm. A straight section is considered to be a *separate crack*. A separate crack whose two ends are connected with other separate cracks is referred to as a *connected crack*, otherwise, as an *isolated crack*. In a series of connected cracks that cross the entire working window, in any direction, each crack is referred to as a *through-connected crack*, otherwise, as a *locally-connected crack*.

The mean two dimensional tortuosity  $T_2$  for the given image is estimated by:

$$T_2 = L_{tc} / L_w N_c \quad (5)$$

where  $N_c$  is the mean number of the intersections of through-connected cracks with a line of length  $L_w$  which is the dimension of the window. This mean number was calculated on the basis of  $i_0$  profiles of the grid.  $L_{tc}$  is the total length of the through-connected cracks, measured within the window.

To obtain data for the estimation of the mean three-dimensional tortuosity  $T_3$ , of a statistically homogeneous and isotropic spatial-crack network, one can use any two-dimensional image of this crack network. Considering cracks in a thin layer of thickness  $h$  one may

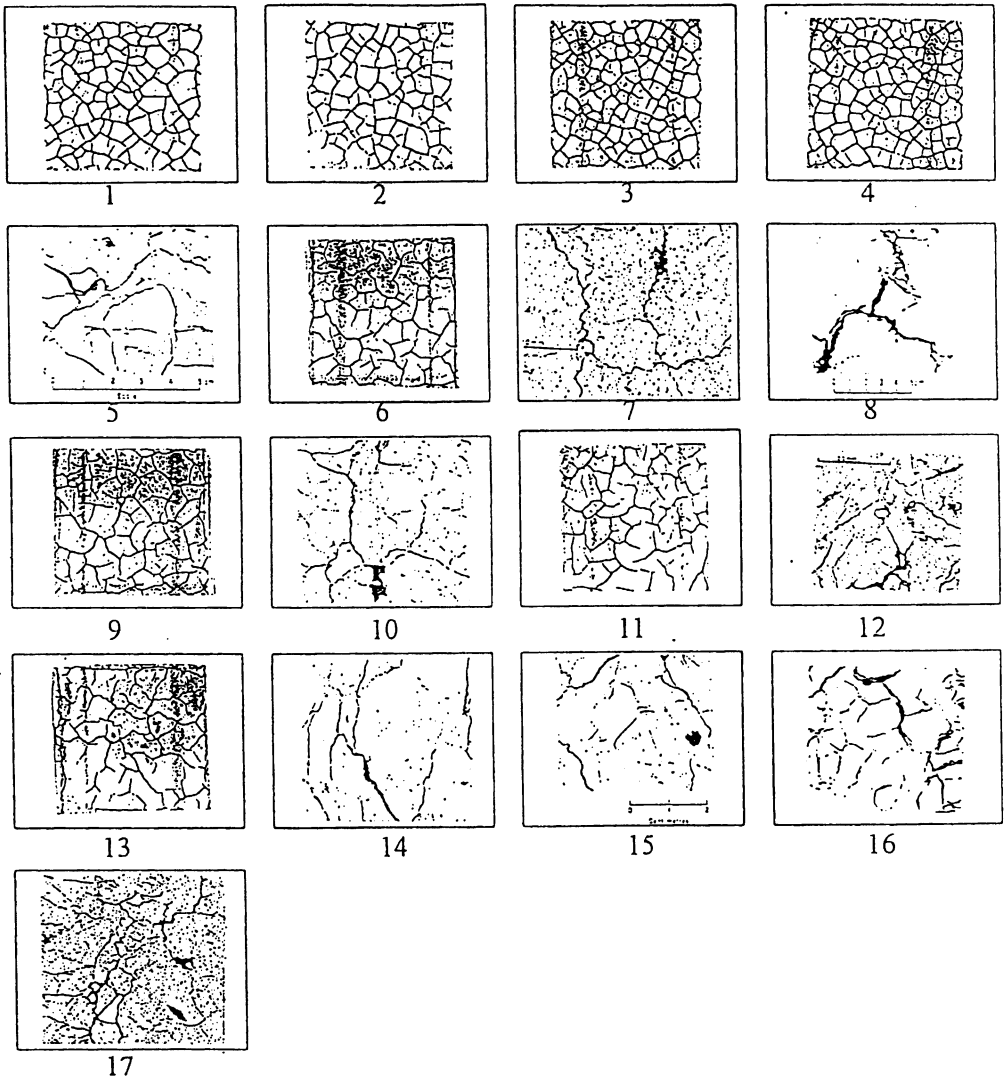


Fig. 2. Two-dimensional crack networks images of clay soils used for experimental estimation of the values  $T_2$  and  $T_3$ .

assume that: 1) the spatial crack network in the layer is statistically homogeneous; and 2) each straight section of length  $l$  of the two-dimensional image of the crack network on the face of the layer corresponds to a plane crack within it. If the angle between the normal to the layer and the crack plane is  $\theta$ , then the surface area of the crack in the layer is equal to  $lh/\cos\theta$ . The total surface area,  $S_{tc}$  of all the through, spatially-connected cracks in the layer is:

$$S_{tc} = \sum_i l_i h / \cos\theta_i \quad (6)$$

where the index  $i$  correspond to a separate straight crack trace in the two dimensional image. According to the definition, the tortuosity of the statistically-homogeneous, spatial-crack network is:

$$T_3 = S_{tc} / L_{tc} h = \left( \sum_i l_i / \cos\theta_i \right) / \left( \sum_i l_i \right). \quad (7)$$

This is the three-dimensional tortuosity in the vicinity of the cross-sectional image under consideration.

For any arbitrary  $i$  th connected crack in the layer the corresponding angle  $\theta_i$  has a random value in the range:

$$0 \leq \theta_i \leq \theta_m \quad (8)$$

where  $\theta_m$  is the maximum possible value of the angle  $\theta_i$ . Herewith  $\theta_m < \pi/2$  because the crack must intersect with the cross-section plane. Before estimating the angle  $\theta_m$  it is worth noting that in the fragment-dimension distribution and the specific fragment surface, any fragment is characterized by its largest dimension  $x$ , only. However, the boundary value  $\theta_m$  of the random values of  $\theta_i$  is determined by geometrical considerations of the mean fragment shape. To define the three dimensions of a fragment of an arbitrary convex shape we consider the two dimensions of its largest face and the dimension normal to the face and designate them, in the order of decreasing values as  $x, y, z$ . The shape of the fragment is characterized by the ratios  $y/x$  and  $z/x$ . The mean fragment shape, that is the mean shape of a set of fragments (outlined by connected cracks), is characterized by the ensemble averages  $\overline{y/x}$  and  $\overline{z/x}$  ( $\overline{z/x} < \overline{y/x} < 1$ ). Defining  $\overline{z/x} \equiv a < 1$  then, if the fragment adjoins the surface of the cross-section from below by its  $(x, y)$  side (Fig. 3), the angle  $\theta_i$ , between the normal to the cross-section,  $n$  and the fragment face (crack) in the layer, can not surpass  $\arctan(x/z)$ , or otherwise must be, on the average, less than  $\arctan(1/a)$ . If the adjoining side is  $(y, z)$  or  $(z, x)$  the limit value of the corresponding angle will be even smaller. Thus:

$$\theta_m = \arctan(1/a). \quad (9)$$

Data from observations by Repin [8], strengthened by theoretical estimates of Chertkov [3] show that for natural rock blocks  $\overline{z/x} \equiv a \approx 0.5$ . This value may be applied to fragments outlined by shrinkage cracks in drying clay soils as shown by Chertkov [4] (it is noteworthy that for soil aggregates this ratio  $\overline{z/x} = 0.63-0.65$  as

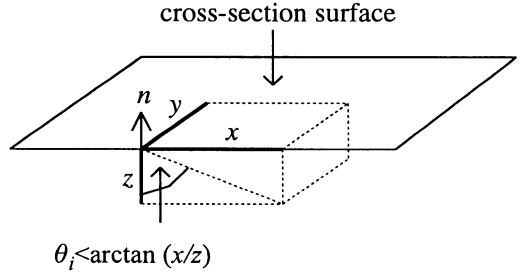


Fig. 3. Sketch for estimating the value of  $\theta_m$ . Values of  $x > y > z$  give the three dimensions of a fragment (ped), of an arbitrary convex shape, adjoining from below to the cross-section surface by the side  $(x, y)$ .  $\theta_i$  is the random angle between the normal to the cross-section and the plane of the  $i$  th crack.

shown by Dexter *et al.* [6] and Dexter [5]. Because of the experimental character of the value  $a \approx 0.5$  one ought to replace  $a$  in Eq. (9) by  $a - 2\sigma$ , where  $\sigma$  is the standard deviation of  $a$  (at a 0.95 confidence level). Since the fragment dimensions were measured to an accuracy of 5-7 % that of their ratio was 10-15 %. Hence,  $a - 2\sigma \approx 0.35$  and:

$$\theta_m \approx \arctan(1/0.35) \approx 70.7^\circ. \quad (10)$$

The procedure for determining the random intersection angle  $\theta_i$  in Eq. (7) is as follows. As a consequence of the crack-network isotropy, it is assumed that the values of the random angle  $\theta_i$  for any  $i$  are uniformly distributed in the range given by Eq. (8). Moduli of the random azimuths  $\varphi_i$  of the crack traces on the cross-sectional plane are also uniformly distributed in the range  $0 \leq |\varphi_i| \leq \pi/2$ . So, we may take as a random value of  $\theta_i$  (if the number of cracks is large):

$$\theta_i = |\varphi_i| \frac{\theta_m}{\pi/2}. \quad (11)$$

In the numerical estimation of the tortuosity  $T_3$ , the angles  $\varphi_i$  were measured relatively to the horizontal side of the working window.

## RESULTS AND DISCUSSION

The results of the estimations of  $T_2$  and  $T_3$  for the crack networks of the images in Fig. 2

are shown by the points in Fig. 1 along with the theoretical line. The numbers correspond to number of the image in Fig. 2.

The experimental errors of  $c$ ,  $T_2$  and  $T_3$  may be estimated as follows. Images 1, 2, 3, and 4 in Fig. 2 are of the same soil and the same conditions [7]. The same is true also for images 6, 9-11, and 13 in Fig. 2 [7] and for images 14 and 15 in Fig. 2 [12]. Hence, it is possible to assess the errors of  $c$ , and for each group of images. The standard deviations  $D_{T_2}$ ,  $D_{T_3}$  found for images 1- 4 are:  $D_{T_2} \cong 0.03$ ,  $D_{T_3} \cong 0.03$ , for images 6, 9, 11, and 13 are:  $D_{T_2} \cong 0.05$ ,  $D_{T_3} \cong 0.09$  and for images 14 and 15 are:  $D_{T_2} \cong 0.03$ ,  $D_{T_3} \cong 0.04$ .

There are three possible sources for the discrepancies between the experimental points and the theoretical curves in Fig. 1:

- the assumption of a square shape for planar fragments and cubic shape for volumetric fragments in the calculations of the mean tortuosities,  $T_2$  and  $T_3$ , respectively;
- the assumption of a statistically-isotropic crack network (equal values of connectedness for the two- and three-dimensional cases and calculating  $T_3$  on the basis of the two-dimensional image);
- the procedure for counting the number of cracks of different types within the working window (the ratio of the crack length to width  $> 3$  and the crack length  $> 2\text{mm}$ ).

One should note with regard to the choice of the fragment shapes that when using two alternative simple fragment shapes - triangle and tetrahedron or circle and sphere - the discrepancies between the theoretical curve of  $T_3$  ( $T_2$ ) and the experimental points in Fig. 1 are much larger and more than three standard deviations. The estimates of the experimental errors of  $T_2$  and  $T_3$  and the distribution of the points around the curves in Fig. 1 show that the discrepancies do not, as a rule, surpass two standard deviations. Hence, one may say that, in spite of the approximations used, results of the suggested model and those of published data of images of crack network in clay soils are in reasonable agreement.

## CONCLUSION

The theoretical estimation of tortuosities of planar and spatial crack networks were based on the relation between cracks and fragments - the faces of fragments are defined by connected cracks. With a statistically-isotropic crack network, the two- and three-dimensional tortuosities,  $T_2$  and  $T_3$ , respectively depend only on the connectedness  $c$  of the crack network and are related to each other. An analytical expression which may be plotted graphically, was found for the function  $T_3(T_2)$ . A method for processing two-dimensional images of crack networks is proposed for estimating the values of  $T_2$  and  $T_3$  (assuming crack network isotropy). Results obtained from seventeen two-dimensional images published in seven works do not contradict the predicted dependency  $T_3(T_2)$ .

## ACKNOWLEDGEMENTS

The research is supported in part by the Israel Ministry of Science and Arts and BARD. V.Y. Chertkov is grateful to the Center for Absorption in Science of the Israel Ministry of Immigrant Absorption for their financial support.

## REFERENCES

1. **Chertkov V.Y.:** Chip development during multiple crack formation in a brittle rock. *Soviet Mining Science*, 21, 489-495, 1986.
2. **Chertkov V.Y.:** Model of fragment formation for short-delay detonation of a series of elongated charges in fissured rock. *Soviet Mining Science*, 22, 447-455, 1987.
3. **Chertkov V.Y.:** Characteristics of the shape of blasted rock fragments. *Soviet Mining Science*, 27, 528-532, 1991.
4. **Chertkov V.Y.:** Mathematical simulation of soil cloddiness. *Int. Agrophysics*, 9, 197-200, 1995.
5. **Dexter A.R.:** Shapes of aggregates from tilled layers of some Dutch and Australian soils. *Geoderma*, 35, 91-107, 1985.
6. **Dexter A.R., Kroesbergen B., Kuipers H.:** Some mechanical properties of aggregates of top soils from the Ijsselmeerpolders. I. Undisturbed soil aggregates. *Neth. J. Agric. Sci.*, 32, 205-214, 1984.
7. **Guidi G., Pagliai M., Petruzzelli G.:** Quantitative size evaluation of cracks and clods in artificially dried soil samples. *Geoderma*, 19, 105-113, 1978.
8. **Repin N.Ya.:** Preparation and excavation of overburden of coal strip mines (in Russian). Moscow, Nedra, p. 256, 1978.

9. **Ringrose-Voase A.J.:** A scheme for the quantitative description of soil macrostructure by image analysis. *J. Soil Sci.*, 38, 343-356, 1987.
10. **Ringrose-Voase A.J., P. Bullock P.:** The automatic recognition and measurement of soil pore types by image analysis and computer programs. *J. Soil Sci.*, 35, 673-684, 1984.
11. **Ringrose-Voase A.J., Nys C.:** One-dimensional image analysis of soil structure. II. Interpretation of parameters with respect to four forest soil profiles. *J. Soil Sci.*, 41, 513-527, 1990.
12. **Scott G.J.T., Webster R., Nortcliff S.:** An analysis of crack pattern in clay soil: its density and orientation. *J. Soil Sci.*, 37, 653-668, 1986.
13. **Scott G.J.T., Webster R., Nortcliff S.:** The topology of pore structure in cracking clay soil. I. The estimation of numerical density. *J. Soil Sci.*, 39, 303-314, 1988.
14. **Velde B., Moreau E., Terribile F.:** Pore networks in an Italian Vertisol: quantitative characterisation by two dimensional image analysis. *Geoderma*, 72, 271-285, 1996.